International Journal of Science and Engineering Applications
Volume 12-Issue 05, 99 - 104, 2023, ISSN:- 2319 - 7560
DOI: 10.7753/IJSEA1205.1028

Thrust Control of Linear Switched Reluctance Motor in Precision Applications

Masoud Karimi
Tabriz University
Tabriz, Iran

Mohammad Bagher Bannae Sharifian
Tabriz University
Tabriz, Iran

Abstract: Linear motors are among the electric machines in which power and linear movement are produced without any mechanical intermediary and directly with the effect of electromagnetic field. Today, among electric drives in manufacturing industries, switched reluctance motors are widely considered due to their lower cost. These motors are one of the most suitable choices for motion control applications with high speed and accuracy. In this research, the goal is to control the linear switched reluctance motor in precise applications. The used model not only reduces the maintenance costs of the collection but also reduces the noise of the entire industry compared to the normal state. First, we control the linear switched reluctance motor with the conventional DTC method, then we improved the desired solution with the fuzzy logic.

Keywords: Switched Reluctance; DTC control; Fuzzy Logic; Linear Motors; Electric motors

1. INTRODUCTION

Due to its exclusive characteristics such as robust and simple mechanical structure, low maintenance, and high reliability and ability to work in harsh environments, Switched Reluctance Motor (SRM) can be considered as an excellent choice for various industrial applications [1-4]. Non-use of winding and permanent magnet in the rotor/translator structure has made it possible to achieve a high speed while the total weight of the motor is also reduced. However, there are some challenges that have prevented their commercial application. One of the main drawbacks of the SRM is high torque/force ripple and significant research has been completed over the last three decades to reduce it using both machine design methods [5,6] and control algorithms [7-11]. Similar to the rotary SRM, the linear switched reluctance motor (LSRM) has many benefits, and the application of this motor could be limited because of its significant force ripple. In addition, using high-precision position control of the LSRM in most motion-control industries is quite important. In this paper, a linear switched reluctance motor with a short primary is used. Linear switched reluctance motors have a simpler construction than other motors and lower maintenance and repair costs. Figure 1. shows the general structure of the linear switched reluctance motor used in this article, which is a 4/6 and three-phase motor.

The force control of the LSRM was proposed in [13] for the first time in which the force ripple of this motor was reduced using the multiphase excitation strategy. In [14], a simple and easy-to-implement position control method was described for high-performance motion of the LSRM in manufacturing automation. The proposed actuator has a simple structure and can be manufactured easily. In order to overcome system perturbations such as system plant parameter variations and the change of operating point, an adaptive control strategy was proposed in [15] for the LSRM. A self-tuning regulator was also developed to combat uncertain control behavior of this motor. By introducing a full-order nonlinear controlled model, the robust passivity based control was proposed in [16] for the position tracking system of the LSRM. To reduce propulsion force pulsations in the LSRM which is essential for elevators, the controlled multiphase excitation using Force Distribution Functions (FDFs) was considered in [17]. To ensure accurate position tracking, a self-tuning regulator based on the pole placement algorithm was developed for the LSRM in [18]. Based on the nonlinear inductance modeling, an improved force distribution function was developed in [19] for the LSRMs to minimize the force ripple.

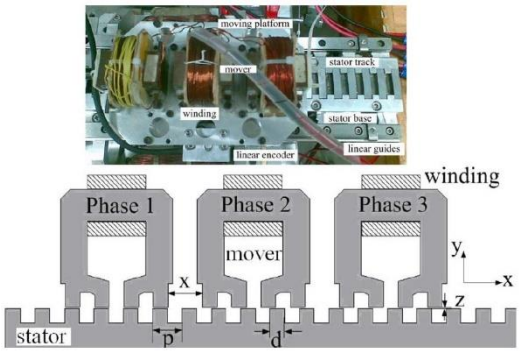

Figure 1. Linear switched reluctance motor prototype [12]

Online parameter estimation using adaptive control strategy was conducted in [20] for the double-sided LSRM to determine system parameter variations and regulate control parameters in real time. Based on instantaneous control of position, speed, current, and force, a control method was introduced in [21] to reduce force ripple of the LSRM. To distribute properly the total force among the phases, a different force distribution function was also proposed in this study.

In order to address limitations related to the previous works in the literature, and with the purpose of accurate control of LSRM in high-precision applications, a novel thrust control method is proposed, which reduces the complexity of the problem modeling using a linear switched reluctance modeling approach.

International Journal of Science and Engineering Applications
Volume 12-Issue 05, 99 - 104, 2023, ISSN:- 2319 - 7560
DOI: 10.7753/IJSEA1205.1028

2. ELECTROMAGNETIC MODELING

One of the serious challenges in the SRMs is the electromagnetic modeling for predicting the dynamic behavior of a motor in different operation conditions. When there is an overlap between stator/rotor poles, the saturation occurs and the characteristics of the flux-linkage will be non-linear. Due to frequent changes from linear to saturation mode, it is complicated to develop an analytical model for the SRM as already. done for induction or synchronous motors. In order to investigate and implement different control methods, an exact model of the motor behavior is required. Various modeling techniques have been introduced for the SRM in the literature and they are generally categorized into 1) linear modeling methods [22], 2) nonlinear modeling methods, and 3) Finite Element Method (FEM) [23-25].

3. STRUCTURE AND MODELING OF LINEAR SWITCHED RELUCTANCE MOTOR

As we know, the behavior and performance of the switched reluctance motor is highly non-linear, which is due to the non-linear behavior of the motor flux [26]. To simplify the motor equations in this paper, we modeled the motor without considering the magnetic saturation of the iron core. With this assumption, the main electrical and mechanical equations of the switched reluctance linear motor will be as follows:

$$u_A = Ri_A + L_0\frac{di_A}{dt} + L_1 cos(\frac{2\pi x}{\lambda})\frac{di_A}{dt} + \frac{2\pi}{\lambda}L_1 sin(\frac{2\pi x}{\lambda})vi_A \quad (3.1)$$

$$u_B = Ri_B + L_0\frac{di_B}{dt} + L_1 cos(\frac{2\pi x}{\lambda} - \frac{2\pi}{3})\frac{di_B}{dt} + \frac{2\pi}{\lambda}L_1 sin(\frac{2\pi x}{\lambda} - \frac{2\pi}{3})vi_B \quad (3.2)$$

$$u_C = Ri_C + L_0\frac{di_C}{dt} + L_1 cos(\frac{2\pi x}{\lambda} - \frac{4\pi}{3})\frac{di_C}{dt} + \frac{2\pi}{\lambda}L_1 sin(\frac{2\pi x}{\lambda} - \frac{4\pi}{3})vi_C \quad (3.3)$$

$$\frac{dv}{dt} = -\frac{\pi L_1}{m\lambda}\left[i_A^2 sin(\frac{2\pi}{\lambda}x) + i_B^2 sin(\frac{2\pi}{\lambda}x - \frac{2\pi}{3}) + i_C^2 sin(\frac{2\pi}{\lambda}x - \frac{4\pi}{3})\right] - \frac{\xi}{m} - \frac{F_C}{m} - \frac{F_0}{m}sign(v) \quad (3.4)$$

In 3.1 to 3.4 u and i, the voltage and current of phases *A*, *B*, *C*, x are equivalent to the location of the linear motor, λ the tooth pitch, F_0 the force caused by the mass of the motor, L_1 and L_0, the minimum and maximum value of inductance, v is velocity, F_c is the load force, m and ξ are load weight and friction. The above relationships are calculated according to the sinusoidal inductance equations of each phase, which are expressed as follows.

$$L_A = L_s + L_m cos(\frac{2\pi}{\lambda} * x) \quad (3.5)$$

$$L_B = L_s + L_m cos(\frac{2\pi}{\lambda} * x - \frac{3\pi}{2}) \quad (3.6)$$

$$L_C = L_s + L_m cos(\frac{2\pi}{\lambda} * x - \frac{4\pi}{2}) \quad (3.7)$$

Figure 2. shows the inductance of each phase of the simulated model. which, like the equations, will be a sinusoidal and alternating waveform. It should be noted that all the electrical and mechanical equations are obtained from the expansion of the inductance equations of each phase.

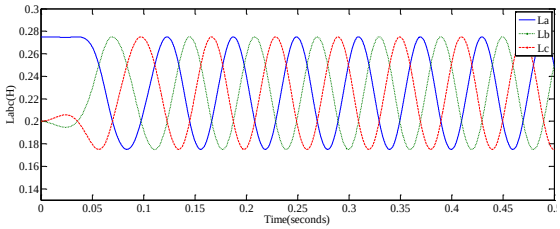

Figure 2. Three phase inductance waveform SRLM

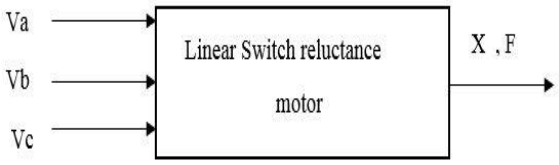

Figure 3. Open loop control of switched reluctance linear motor

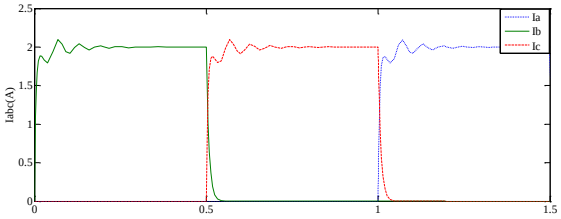

Figure 4. Three phase current in open loop control

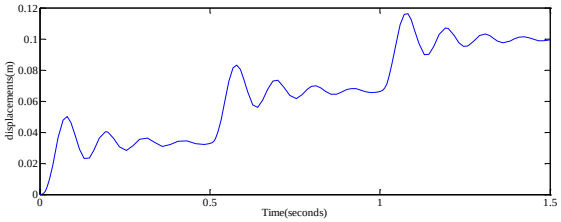

Figure 5. location of LSRM as a function of time for three steps

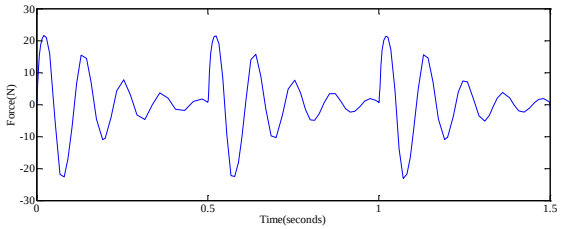

Figure 6. Dynamic force as a function of time for three steps

3.1 Open loop control system

Open circuit control is a simple method. In such a system, the motor phases are fed in a specific order based on the location recorded in the reference value of the phases, so there is no feedback loop. In fact, as seen in Figure 5. We have no control over the flux and other parameters of the motor. According to figures 3 to 6, it can be concluded that the ripple of the linear motor is high in this method, so we will use other methods to reduce the ripple.

International Journal of Science and Engineering Applications
Volume 12-Issue 05, 99 - 104, 2023, ISSN:- 2319 - 7560
DOI: 10.7753/IJSEA1205.1028

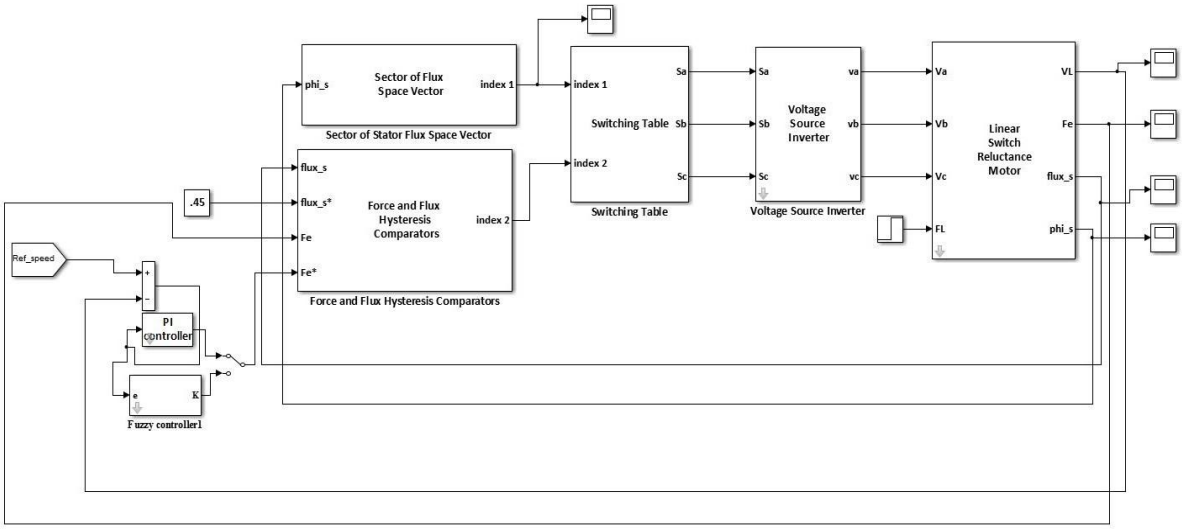

Figure 7. Simulated overview in MATLAB environment

3.2 Simulation results using DFC method

Investigating the performance of the linear reluctance switch motor in steady state is the main performance characteristic for the motor, and in this case, the condition is checked that the system has passed all its transient states. These conditions may be due to changes in load torque, stator reference flow and even changes in motor voltage to check its effect on system dynamics. Figure 7. shows the general scheme of the DTC controller applied to the linear switched reluctance motor, with the of a switch, the set can be converted from the conventional PI mode to the fuzzy logic control mode.

Table 1 shows the general specifications of the LSRM in question and the values of the parameters set to check the performance of the LSRM in steady state.

According to figure 8. Fluxes, like current, are alternating and symmetrical in all phases. Controlling the flux at a constant speed causes the stator flux vector to move at a constant average speed. This issue causes a uniform and alternating time distribution of the current and flux of the winding phases. On the other hand, since the power and flow of the motor are directly controlled by the hysteresis band, the currents of the stator phases have many harmonic components. In fact, the voltage is applied to the stator phases through the switching devices and based on the momentary values of the power and flow of the motor.

Figure 9 shows the tracking of the reference flux by the control system. As it is clear from the above figure, the amount of flux ripple is minimal, and the accuracy and speed in tracking the reference flux is appropriate.

Table 1. Specifications of the simulated linear motor

U=30 V	D φ^*_s =0.45 (H)
L_0 = 225 mH	$bw-\varphi_s$ =0.009 (wb)
L_1 = 50 mH	$bw-F_s$ =0.3(N)
R = 18 ohm	F_0 = 0.2 N
M = 5 Kg	ξ =75 N/s
λ = 10 mm	

Figure 10 shows the routing of the stator flux, which according to the figure reached the value of 0.45 on each side and formed a circle. In fact, this figure is obtained from the orthogonal axes used to calculate the size and angle of the stator flux.

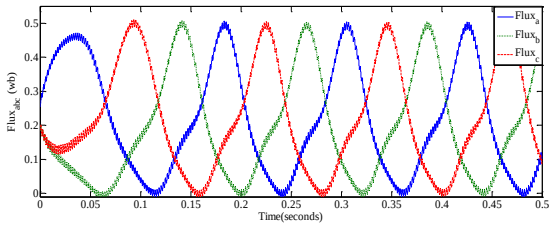

Figure 8. Flux of three-phase linear switched reluctance motor in steady state

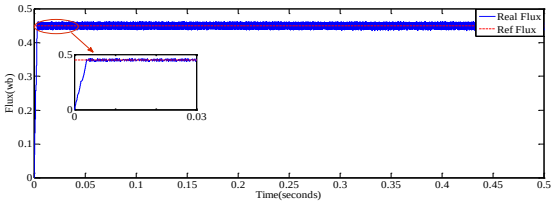

Figure 9. Flux of three-phase linear switched reluctance motor in steady state

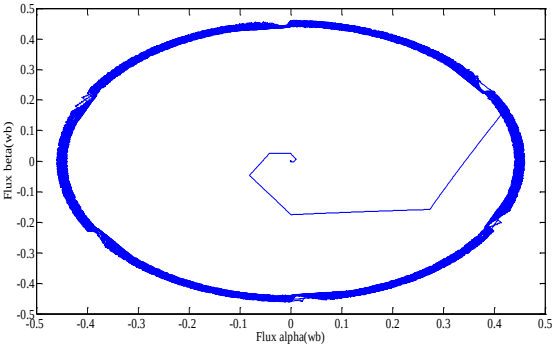

Figure 10. Flux of three-phase linear switched reluctance motor in steady state

International Journal of Science and Engineering Applications
Volume 12-Issue 05, 99 - 104, 2023, ISSN:- 2319 - 7560
DOI: 10.7753/IJSEA1205.1028

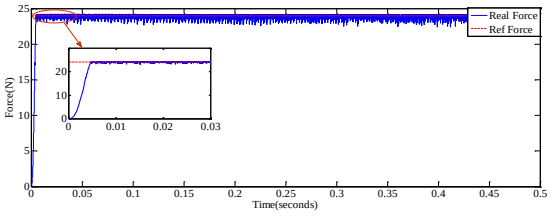

Figure 11. Three-phase Force and reference force of LSR motor

Figure 11. The total force has followed the reference force which is the output of the PI controller with proper accuracy.

4. INVESTIGATING THE EFFECT OF LOAD FORCE ON THE FLUX OF LSRM

As we know, one of the advantages of the DTC control method is the lack of dependence between flux and power. For this purpose, we increase the desired force from 5 (N) to 30 (N) so that the flux can be seen more clearly in case of changes.
According to Figure 12. and Figure 13. It is quite evident that force changes have no effect on the total stator flux and this is one of the most important advantages of the DTC method. In the case of the three-phase motor, it can be said that at the moment of changing the flow of the motor, there is no adverse effect on the force. In other words, motor flow control is independent of its force.

4.1 End effect and its effect on speed and force

The effect of the end effect on the force decreases with the increase in the number of moving poles. The end effect in the linear switched reluctance motor shows its effect more by increasing the speed, in such a way that by weakening the flux in the phases, it reduces the amount of power that can be produced in them. The decrease in the production force in the engine causes an increase in the speed ripple compared to the normal state, which we will explain below. Also, the maximum amount of load that can be tolerated in this case will be reduced due to the reduction of power. Figure 15. shows the three-phase power of the LSR motor considering 5% of the final effect in the phases of the LSR motor.
Figure 15 shows the speed of the LSR motor considering the end effect. Due to the reduction of the force of each phase, the

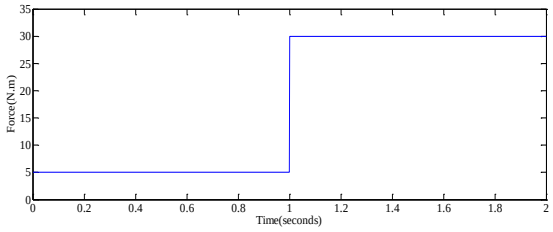

Figure 12. Step changes of force

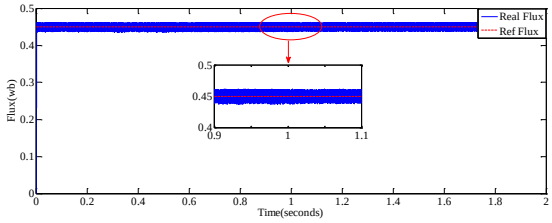

Figure 13. Total stator flux at the moment of force changes

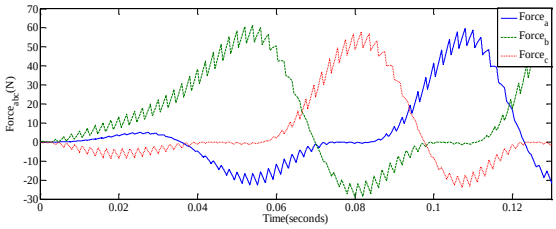

Figure 14. The force of each phase in LSRM

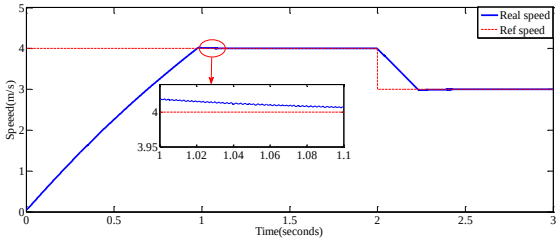

Figure 15. LSRM speed with end effect

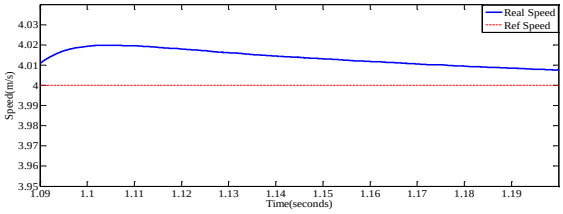

Figure 16. LSRM speed with end effect

speed ripple increases compared to the initial speed, which can be seen by comparing with the normal state in Figure 17. It should be noted that the end effect is more visible at high speeds.

5. SPEED CONTROL IN LSRM

In this section, we use two methods to follow the reference speed. The first method is to use the PI controller to get an acceptable response for the actual speed of the motor. It should be noted that the coefficients are different for each engine with different parameters, which makes it difficult to determine the coefficients. The second method is fuzzy control, which has higher accuracy for speed tracking, in fact, fuzzy logic is a smart method to reduce the dependence on engine parameters and get a much better response from the output. In the following, we will examine the results obtained in two methods.

5.1 Conventional PI method

In this method, after calculating the PI coefficients, we reach our desired answer with trial and error or any algorithm. As can be seen in Figure 18, in the conventional method, when converging, at each stage, we will first have an overshoot and then a downshoot, which causes an increase in the shock

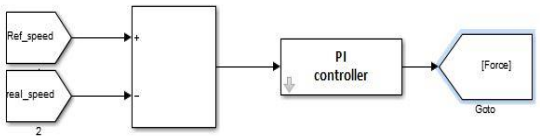

Figure 17. Conventional method of PI controller

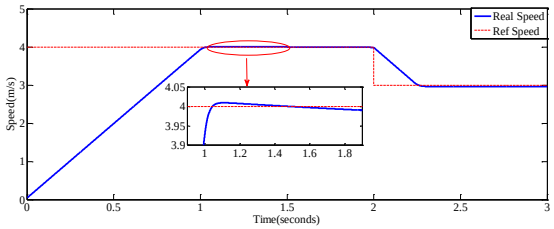

Figure 18. Conventional method of PI controller

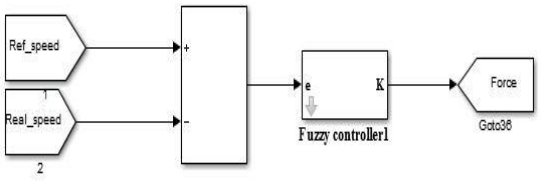

Figure 19. Fuzzy logic

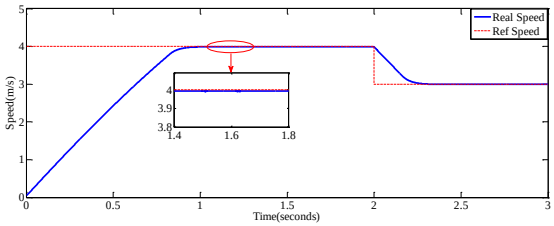

Figure 20. Fuzzy logic

applied to the engine, this type of shock is also a type of ripple. is Successive shocks to the engine also have their own problems that reduce the life of the engine and cause errors in the system's performance in precise applications.

5.2 Fuzzy control method

According to Figure 20, in this type of controller, we will not have any overshoot or undershoot, and the motor will reach its real speed much smoother. In fact, with the fuzzy logic, the shocks at the beginning of convergence have been eliminated, and the motor can continue to move more accurately in certain applications. The engine will also have a lot of influence, because of which this method will be more suitable than the conventional method.

6. CONCLUSION

This paper is focused on the control of the linear switched reluctance motor in high precision applications, and the direct power control method has been used to achieve this goal. After introducing the SR linear motor and the necessary preparations to understand how it works, different methods used in the design of linear switched reluctance motor drivers are proposed. Since the developed high precision control method is economical due to its novel structure, it can be utilized for various applications by changing the reference speed.

REFERENCES

[1] Todd, R., Valdivia, V., Bryan, F. J., Barrado, A., Lázaro, A., & Forsyth, A. J. (2014). Behavioural modelling of a switched reluctance motor drive for aircraft power systems. *IET Electrical Systems in Transportation*, *4*(4), 107-113.

[2] Zhu, J., Cheng, K. W. E., Xue, X., & Zou, Y. (2017). Design of a new enhanced torque in-wheel switched reluctance motor with divided teeth for electric vehicles. *IEEE Transactions on Magnetics*, *53*(11), 1-4.

[3] Mishra, A. K., & Singh, B. (2017). Solar photovoltaic array dependent dual output converter based water pumping using switched reluctance motor drive. *IEEE Transactions on Industry Applications*, *53*(6), 5615-5623.

[4] Wang, D., Wang, X., & Du, X. F. (2017). Design and comparison of a high force density dual-side linear switched reluctance motor for long rail propulsion application with low cost. *IEEE Transactions on Magnetics*, *53*(6), 1-4.

[5] Sahin, C., Amac, A. E., Karacor, M., & Emadi, A. (2012). Reducing torque ripple of switched reluctance machines by relocation of rotor moulding clinches. *IET Electric Power Applications*, *6*(9), 753-760.

[6] Ma, C., & Qu, L. (2015). Multiobjective optimization of switched reluctance motors based on design of experiments and particle swarm optimization. *IEEE Transactions on Energy Conversion*, *30*(3), 1144-1153.

[7] Ye, J., Bilgin, B., & Emadi, A. (2015). An offline torque sharing function for torque ripple reduction in switched reluctance motor drives. *IEEE Transactions on energy conversion*, *30*(2), 726-735.

[8] Deng, X., Mecrow, B., Wu, H., & Martin, R. (2017). Design and development of low torque ripple variable-speed drive system with six-phase switched reluctance motors. *IEEE Transactions on Energy Conversion*, *33*(1), 420-429.

[9] Kazemtarghi, A., Chandwani, A., Ishraq, N., & Mallik, A. (2022). Active Compensation-based Harmonic Reduction Technique to Mitigate Power Quality Impacts of EV Charging Systems. *IEEE Transactions on Transportation Electrification*.

[10] Naghizadeh, M., Gohari, H. S., Hojabri, H., & Muljadi, E. (2022). New Single–Phase Three-Wire Interlinking Converter and Hybrid AC/LVDC Microgrid. *IEEE Transactions on Power Electronics*.

[11] Kazemtarghi, A., Dey, S., Mallik, A., & Johnson, N. G. (2023). Asymmetric Half-Frequency Modulation in DAB to Optimize the Conduction and Switching Losses in EV Charging Applications. *IEEE Transactions on Transportation Electrification*.

[12] Krishnan, R. (2017). *Switched reluctance motor drives: modeling, simulation, analysis, design, and applications*. CRC press.

[13] Bae, H. K., Lee, B. S., Vijayraghavan, P., & Krishnan, R. (2000). A linear switched reluctance motor: converter and control. *IEEE Transactions on Industry Applications*, *36*(5), 1351-1359.

[14] Gan, W. C., Cheung, N. C., & Qiu, L. (2003). Position control of linear switched reluctance motors for high-precision applications. *IEEE Transactions on Industry Applications*, *39*(5), 1350-1362.

[15] Lim, H. S., & Krishnan, R. (2007). Ropeless elevator with linear switched reluctance motor drive actuation systems. *IEEE transactions on industrial electronics*, *54*(4), 2209-2218.

[16] Zhao, S. W., Cheung, N. C., Gan, W. C., Yang, J. M., & Zhong, Q. (2008). Passivity-based control of linear switched reluctance motors with robustness consideration. *IET Electric Power Applications*, *2*(3), 164-171.

[17] Lim, H. S., Krishnan, R., & Lobo, N. S. (2008). Design and control of a linear propulsion system for an elevator using linear switched reluctance motor drives. *IEEE transactions on industrial electronics*, *55*(2), 534-542.

[18] Zhao, S. W., Cheung, N. C., Gan, W. C., & Yang, J. M. (2010). High-precision position control of a linear-switched reluctance motor using a self-tuning regulator. *IEEE transactions on power electronics*, *25*(11), 2820-2827.

[19] Pan, J. F., Cheung, N. C., & Zou, Y. (2012). An improved force distribution function for linear switched reluctance motor on force ripple minimization with nonlinear inductance modeling. *IEEE transactions on magnetics*, *48*(11), 3064-3067.

[20] Pan, J. F., Zou, Y., & Cao, G. (2013). Adaptive controller for the double-sided linear switched reluctance motor based on the nonlinear inductance modelling. *IET Electric Power Applications*, *7*(1), 1-15.

[21] Masoudi, S., Feyzi, M. R., & Banna Sharifian, M. B. (2016). Force ripple and jerk minimisation in double sided linear switched reluctance motor used in elevator application. *IET Electric Power Applications*, *10*(6), 508-516.

[22] Kazemtarghi, A., Dey, S., & Mallik, A. (2022). Optimal Utilization of Bidirectional EVs For Grid Frequency Support in Power Systems. *IEEE Transactions on Power Delivery*.

[23] Ganji, B., & Askari, M. H. (2016). Analysis and modeling of different topologies for linear switched reluctance motor using finite element method. *Alexandria Engineering Journal*, *55*(3), 2531-2538.

[24] Wang, D., Du, X., Zhang, D., & Wang, X. (2017). Design, optimization, and prototyping of segmental-type linear switched-reluctance motor with a toroidally wound mover for vertical propulsion application. *IEEE transactions on industrial electronics*, *65*(2), 1865-1874.

[25] Chandwani, A., Kazemtarghi, A., & Mallik, A. (2022, March). Quantification and Active Filtering-based Mitigation for Third Harmonic Component Attenuation in Totem-pole PFC for Onboard Charging Systems. In *2022 IEEE Applied Power Electronics Conference and Exposition (APEC)* (pp. 1170-1175). IEEE.

[26] Inderka, R. B., & De Doncker, R. W. (2003). DITC-direct instantaneous torque control of switched reluctance drives. *IEEE Transactions on Industry Applications*, *39*(4), 1046-1051.